OAK RIDGE
NATIONAL LABORATORY
MANAGED BY UT-BATTELLE
FOR THE DEPARTMENT OF ENERGY

ORNL/TM-2009/210

Passive and Active Fast-Neutron Imaging in Support of AFCI Safeguards Campaign

August 2009

Prepared by
Paul Hausladen and
Matthew Blackston

UT-BATTELLE
ORNL-27 (4-00)

ORNL/TM-2009/210

Global Nuclear Security Technology Division

PASSIVE AND ACTIVE FAST-NEUTRON IMAGING IN SUPPORT OF AFCI SAFEGUARDS CAMPAIGN

Paul Hausladen and Matthew Blackston

August 2009

Prepared by
OAK RIDGE NATIONAL LABORATORY
Oak Ridge, Tennessee 37831-6283
managed by
UT-BATTELLE, LLC
for the
U.S. DEPARTMENT OF ENERGY
under contract DE-AC05-00OR22725

CONTENTS

Page

LIST OF FIGURES

ACKNOWLEDGMENTS

The experiments described in this report were performed with collaborators from the Idaho National Laboratory (INL). INL collaborators included D. Chichester, J. Johnson, and S. Watson. The work in this report was sponsored by the Department of Energy AFCI Safeguards Campaign. The coded-aperture fast-neutron imager used in the present work was recently assembled and tested using funding from the Laboratory Directed Research and Development Program of Oak Ridge National Laboratory, managed by UT-Battelle, LLC, for the U. S. Department of Energy.

ABSTRACT

Results from safeguards-related passive and active coded-aperture fast-neutron imaging measurements of plutonium and highly enriched uranium (HEU) material configurations performed at Idaho National Laboratory's Zero Power Physics Reactor facility are presented. The imaging measurements indicate that it is feasible to use fast neutron imaging in a variety of safeguards-related tasks, such as monitoring storage, evaluating holdup deposits in situ, or identifying individual leached hulls still containing fuel. The present work also presents the first demonstration of imaging of differential die away fast neutrons.

INTRODUCTION

This letter reports results from ORNL passive and active fast-neutron imaging measurements performed as part of Advanced Fuel Cycle Initiative (AFCI) Safeguards Campaign work package OR09150040314, "ORNL Active Interrogation." The measurements performed under the auspices of this work package consist of a combination of commissioning and calibration measurements for a newly developed coded-aperture fast-neutron imager at ORNL and imaging measurements with safeguards-related neutron sources of plutonium and highly enriched uranium (HEU) at the Idaho National Laboratory (INL) Zero Power Physics Reactor (ZPPR) facility. The measurements were undertaken to demonstrate this new capability of coded-aperture fast-neutron imaging, both passively with spontaneous fission sources and actively with induced fission sources, and to evaluate the capability in the context of safeguards-related scenarios. Fast-neutron imaging is appealing in scenarios where contact measurements with non-imaging detectors may be impractical or too labor intensive, or their results ambiguous because of surrounding material. In combination with active interrogation, fast-neutron imaging measurements can make non-contact determination of fissile mass. Coded-aperture fast-neutron imaging is appealing, compared with neutron scatter cameras, because the spatial resolution is sufficient to separate individual process lines or containerized sources in storage from a distance, or to enable diagnostic measurements of the distribution of fissile material in an instance of holdup.

THE ORNL FAST-NEUTRON IMAGER

Because of both the diagnostic nature of fission-spectrum neutron emissions and their ability to penetrate objects opaque to gamma radiation, fast-neutron imaging can be applied to a variety of safeguards-related scenarios. Coded-aperture imaging offers the opportunity to measure with a combination of good spatial resolution and efficiency. The most common variant of the coded-aperture technique replaces the pinhole aperture from a pinhole imager with a cleverly chosen array of pinholes (a coded aperture) such that the image can be uniquely reconstructed from the modulated signal on the detectors; the large open area of such an aperture decreases the time needed to image a point source by the square root of the number of open holes in the coded aperture. Coded-aperture imagers were originally developed by the astronomical community in the 1980s and are well established in gamma-ray astronomy; more recently, they have been applied to terrestrial gamma ray and thermal neutron based arms-control and homeland security applications [1–4]. The present work provides the first steps toward evaluating the capability of coded-aperture imaging of fast neutrons for safeguards-related applications, particularly when combined with active interrogation.

The ORNL fast-neutron imager used in the present measurements consists of 25 fast plastic neutron and gamma ray detectors each containing 100 individual pixels. Arranged in a 5 × 5 array, the detectors comprise a 54 × 54 cm panel of 2500 pixels. The pixilated neutron detectors were developed at ORNL for fast-neutron imaging, and each consists of a 10 × 10 array of 1.07 × 1.07 × 5 cm scintillator pixels backed by a light guide viewed by four photomultiplier tubes whose shared response determines the pixel of interaction [5]. The detector panel is read out by a data acquisition adapted from a Siemens Inveon Preclinical Positron Emission Tomography (PET) medical imaging system, which calculates the interaction pixel of each detector count in hardware and timestamps each count with 0.312 ns resolution. The acquisition system is scalable to a large number of detectors, and in the present configuration, only 25 of 64 available slots were used. The detector array was originally developed (and still used) for fast-neutron and induced fission transmission imaging. The detector array was repurposed to a coded-aperture imager with the addition of a base-19 modified uniformly redundant array (MURA) high-density polyethylene

coded-aperture mask and detector fixture that included 2.54 cm of lead gamma ray shielding. Since the fast-plastic scintillation detectors are sensitive to neutrons and gamma rays, the combination of a polyethylene mask that poorly modulates gamma rays and substantial lead shielding that shields the detectors from gamma rays serves to minimize the sensitivity of the imager to gamma rays. While imperfect compared with detectors that can distinguish neutrons from gamma rays, the fast-neutron and gamma ray detectors were available to be borrowed and sufficient for demonstration of the technique. A photograph of the imaging system configured for coded-aperture imaging is shown with a mask pattern whose smallest element is 1.4 cm in Fig. 1.

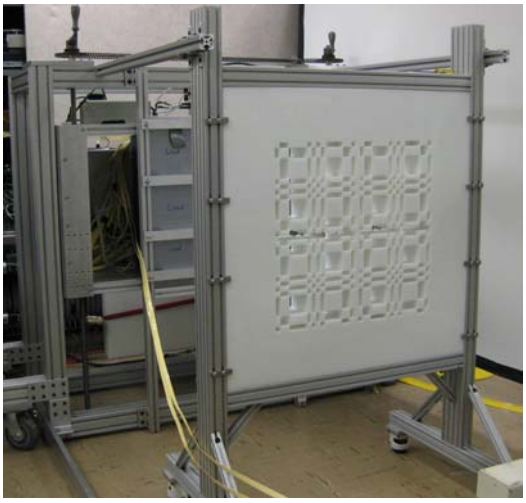

Fig. 1. The ORNL coded-aperture fast-neutron imager. The high density polyethyleme base-19 MURA coded-aperture mask is visible in the foreground, and the lead shielding in front of the detector plane is visible in the background.

Calibration measurements were performed with an instrumented ^{252}Cf fission chamber which provides a time-of-flight start from detection of each fission event. Fission gamma rays and neutrons from the source were then identified via their characteristic times of flight. One such measurement is shown in Fig. 2 for neutrons (top) and gamma rays (bottom) on the same intensity scale. The left-most image shows the distribution of counts in the detector showing modulation from the coded-aperture mask, and the middle image shows its corresponding reconstruction. The right-most plot shows the projection of the reconstruction and the corresponding fit to a Gaussian distribution to determine the imaging resolution to be 3.6 cm full width at half maximum (FWHM) at the imaging plane, or about 1° angular resolution. The imager sees about 4 times the signal from neutrons per fission as gamma rays. Taking into account the differing fission neutron and gamma ray multiplicities, the sensitivity per fission gamma is about 12 percent that per fission neutron.

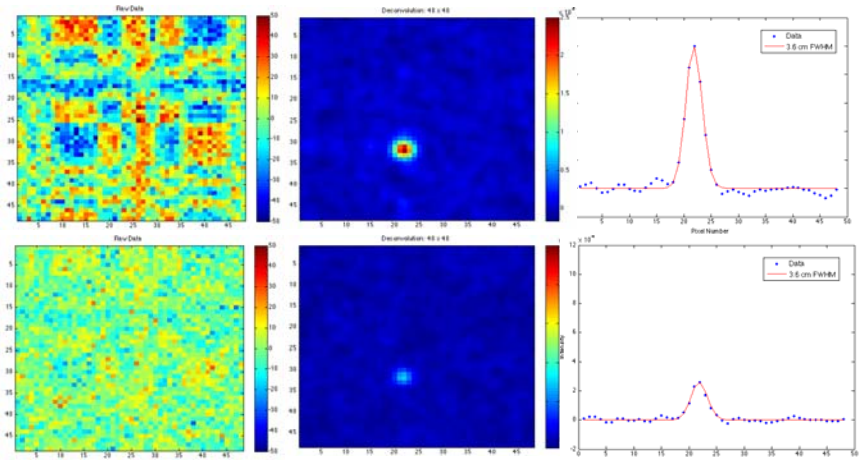

Fig. 2. From left to right, detector data showing the spatial modulation from projection of the mask on the detectors, reconstructed image, and projection onto x-axis with Gaussian fit for (top) fission neutrons and (bottom) fission gamma rays on the same image scale.

The mask and detector fixture to convert to a coded-aperture imaging system were designed and built and the imager was tested using a small amount of support from the ORNL Laboratory-Directed Research and Development Fund. The substantial investment of the imaging array was leveraged in the present work to measure safeguards-related neutron and gamma rays sources at the INL ZPPR facility as well as to undertake the first active fast-neutron die-away imaging measurements with fissile material.

PASSIVE IMAGING MEASUREMENTS

Measurements with fissile materials were performed at the INL ZPPR facility, where it was possible to access and use material from the ZPPR fissile material storage vault. Passive measurements of plutonium mixed oxide (MOX) fuel pins were performed in two configurations, one a "soup can" containing 90 fuel pins that fill the can to capacity, and another a "clamshell" containing nine pins arranged three deep in the form of an "I". Each 3/8 in. by 6 in. Vendor 80 Type 129 fuel pin contains 3.66 g ^{240}Pu, which emits about 3700 neutrons s^{-1} for a total of 3.33×10^5 and 3.33×10^4 neutrons s^{-1}, respectively, in the two configurations. The configurations of the fuel pins are shown in Fig. 3.

Measurements included both detailed close-up measurements where the material was positioned 1 m from the coded-aperture mask (2 m from the detector), and more distant measurements, where the material was positioned 5 m from the coded-aperture mask (6 m from the detector). For the close-up measurements, a mask pattern based on a 1.4 cm smallest element was used to maximize resolution, and both configurations of fuel pins were used. For the more distant measurements, a mask pattern based on a 2 cm smallest element gave a larger field of view, and only the soup-can fuel configuration was used. In both cases, the mask was 10 cm thick, which corresponds to about one attenuation length of fast neutrons, to maximize contrast. The intrinsic efficiency of the array with no mask in place was measured for ^{252}Cf fission neutrons to be 0.164 with no lead shielding and 0.138 with lead shielding in place. The close-up "characterization" imaging measurements could be envisioned to be used in safeguards-related scenarios to obtain detailed geometrical information of a holdup deposit where it was necessary to know the geometry of the deposit in order to properly measure its fissile mass in situ. Such measurements also could be used to pinpoint the location of fissile material with high accuracy,

such as to identify a particular hull cladding that still contains fuel after leaching. Imaging measurements at longer distances may be useful in monitoring process lines, storage, or material movement. Table 1 summarizes the passive measurement configurations, times, and signal rates. Note that these counting rates are small compared with the overall background rate in the imaging detector of 1300 s^{-1} with no sources present in the workroom. This rate is indicative of the high-background environment at the ZPPR and is an important consideration in coded-aperture imaging where the uncertainty in each pixel equals the uncertainty in the total counts in the detector.

Fig. 3. Configurations of plutonium MOX fuel for the passive imaging measurements. The clamshell on the left contains a total of nine pins in a three-deep "I" formation. The soup can on the right contains 90 pins.

Note that the calculations of neutron rates from the fuel (assuming no self-attenuation) using the known solid angle and efficiency of the imaging array indicate that the gamma component comprises the majority of counts.

Table 1: Summary of passive measurements with Pu fuel configurations

Measurement	Distance	Time	Signal	Neutron Rate
"I" configuration	2 m	120 min	59 s^{-1}	8.3 s^{-1}
Soup can (vertical)	2 m	30 min	384 s^{-1}	83 s^{-1}
Soup can (horizontal)	2 m	40 min	250 s^{-1}	83 s^{-1}
Soup can on far table	6 m	40 min	33 s^{-1}	8.7 s^{-1}
Soup can on floor behind "wall"	6 m	90 min	18 s^{-1}	8.7 s^{-1}

Note that the known source strength and the solid angle and efficiency of the imaging array allow the true neutron rate (assuming minimal self-attenuation) to be calculated. These rates indicate that the majority of signal for these aging plutonium MOX fuels originates from gamma rays even through the lead shielding. In contrast, for fission neutrons and gamma rays from a ^{252}Cf fission source, three-quarters of the signal originates from neutrons.

Photographs and mixed neutron/gamma images from the close-up configurations are shown in Fig. 4. The 3.6 cm resolution of the imaging system to fission neutrons in the object plane is sufficient to resolve the individual pins in the "I" configuration as well as the orientation and dimensions of the soup can.

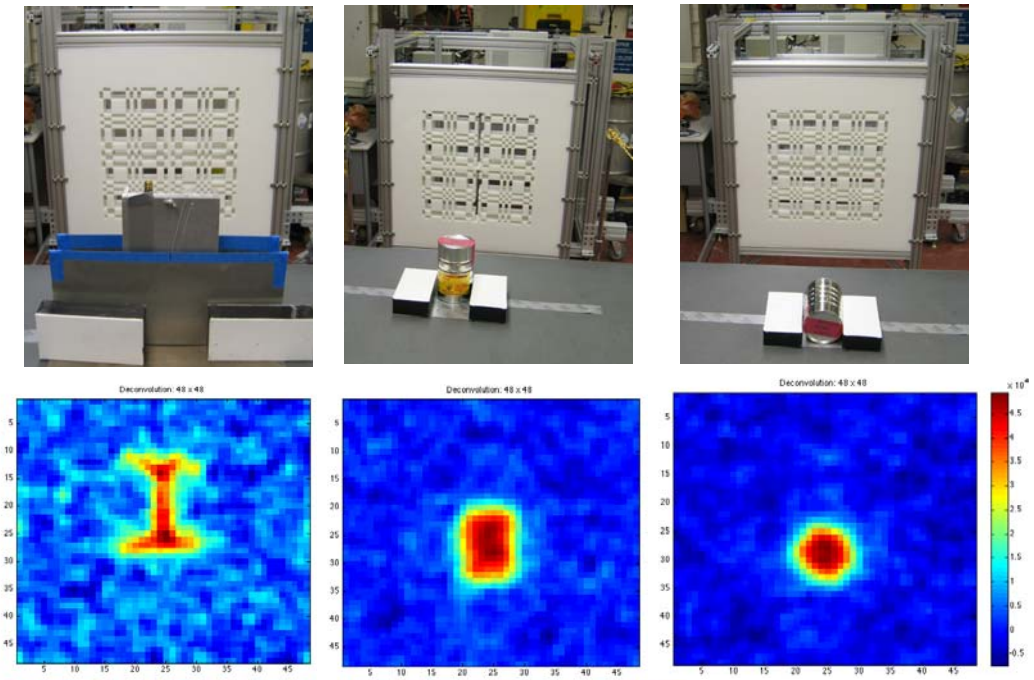

Fig. 4. Photographs of imaging configuration along with coded-aperture neutron-gamma images for (left) the clamshell with the "I" configuration, (middle) the soup can standing vertically, and (right) the soup can laying horizontally.

Provided the solid angle, source strength, and efficiencies are known, measurement time to reach a specified signal to noise N_σ can be calculated from

$$t = \left(\frac{N_\sigma}{0.5 s_0 \varepsilon (1-T)} \right)^2 (b_0 + s_0 \varepsilon T + 0.5 s_0 \varepsilon (1-T)),$$

where t is the time in seconds, N_σ is the desired signal to noise in standard deviations, s_0 is the source rate incident on the detector, ε is the intrinsic efficiency of the detector, T is the fraction of neutrons that transmits through the solid portion of the mask, and b_0 is the background rate in the detector. Note that the denominator of the squared quantity is simply the signal rate in the detector and the quantity starting with b_0 is simply the total count rate in the detector from background, unmodulated source counts, and signal counts. The time required to detect the presence of the "I" configuration to 5 standard deviations if the counts were all in a single pixel would be about 10 s. However, the signal strength associated with each pixel is only a few percent of the total and measurement time scales like the inverse-square of the signal strength. Consequently, diagnostic measurements such as this tend to be long but can be shortened by eliminating the gamma ray count rate from the detectors. Since measurement time is proportional to background and the background is overwhelmingly gamma, measurement time can in principle be shortened 2 (or more) orders of magnitude using detectors that can distinguish neutrons from gamma rays. However, because the measured signal in these scoping measurements is primarily gamma, the gain in measurement speed for these objects would be less: approximately a factor of 3 shorted for the soup can, and approximately no change for the "I" geometry. Measurement time to find a single 5 cm segment of a fuel pin (assuming a neutron source strength that is a third of the 3700 n s^{-1} for the 15 cm pins used in this study) still containing its fuel among leached hulls would be about 45 min with the present measurement geometry and a background rate of 10 neutrons s^{-1}. This time could be shortened substantially by fairly simple improvements; for

example, the measurement time could be approximately halved by changing the mask material or thickness to correspond to two mean paths rather than a single mean free path.

Coded-aperture imaging is best suited to measurements of point sources, and in fact for measurements with the longer source-to-detector distance of 6 m, the soup can source appears pointlike. Photographs and mixed neutron/gamma images from the more distant configurations are shown in Fig. 5. Note that while these measurements were lengthy, much shorter measurements are possible. For the soup can on the table, the detected image is approximately 11 standard deviations above background fluctuations, much more than required to detect its presence. In addition, liquid scintillator detectors that can discriminate between neutrons and gamma rays would reduce background to the point that 5σ detection would be possible in approximately 10 s. Similarly, the "soup can" behind the wall can be detected to five standard deviations using approximately 100 s of data from the present measurements. Using neutrons only (assuming 50% of neutrons pass through the wall and a background of 10 counts s^{-1}), the same measurement could be performed in approximately 25 s. These results suggest that it is conceivable that longer-dwell measurements could monitor storage configurations even through walls.

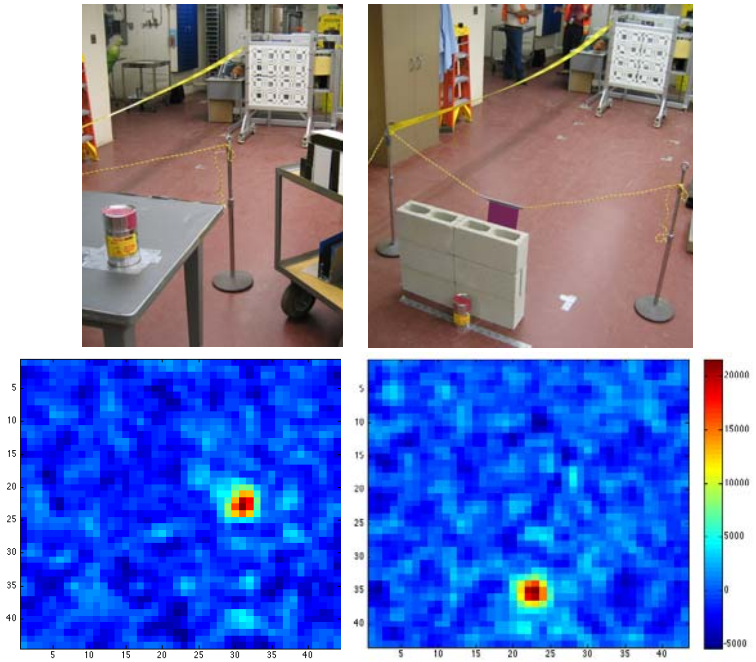

Fig. 5. Photographs of imaging configuration along with coded-aperture neutron-gamma images for (left) soup can on table at 6 m and (right) soup can behind cinderblock wall at 6 m.

ACTIVE IMAGING MEASUREMENTS

Active measurements were performed on 9.428 kg of HEU metal plates containing 8.785 kg of ^{235}U in a clamshell. The ^{235}U fuel emits nearly no neutrons spontaneously, so fissions were induced in the material via active interrogation with neutrons from a Thermo Electron MP320 electronic deuterium-tritium (D-T) neutron generator. The source produces a monoenergetic neutron spectrum of 14 MeV and a maximum intensity of approximately 2×10^8 neutrons s^{-1}. For the measurements, the D-T generator was operated at 300 pulses s^{-1} at 10% duty cycle and maximum output, so the instantaneous output during the interrogation pulse was approximately 2×10^9 neutrons s^{-1}. The clamshell containing HEU was positioned near the D-T generator and

surrounded by high-density polyethylene moderator on three sides, as shown in the photograph in Fig. 6. Moderated neutrons from the D-T generator pulse diffuse from the moderator into the clamshell between D-T generator pulses to induce fissions and create the conventional differential die-away signal. The time dependence of the total counts in the imager with respect to the interrogating pulse time are shown at the left in Fig. 6. The time regions used to image the D-T source and the HEU die away are also indicated and the resulting images shown.

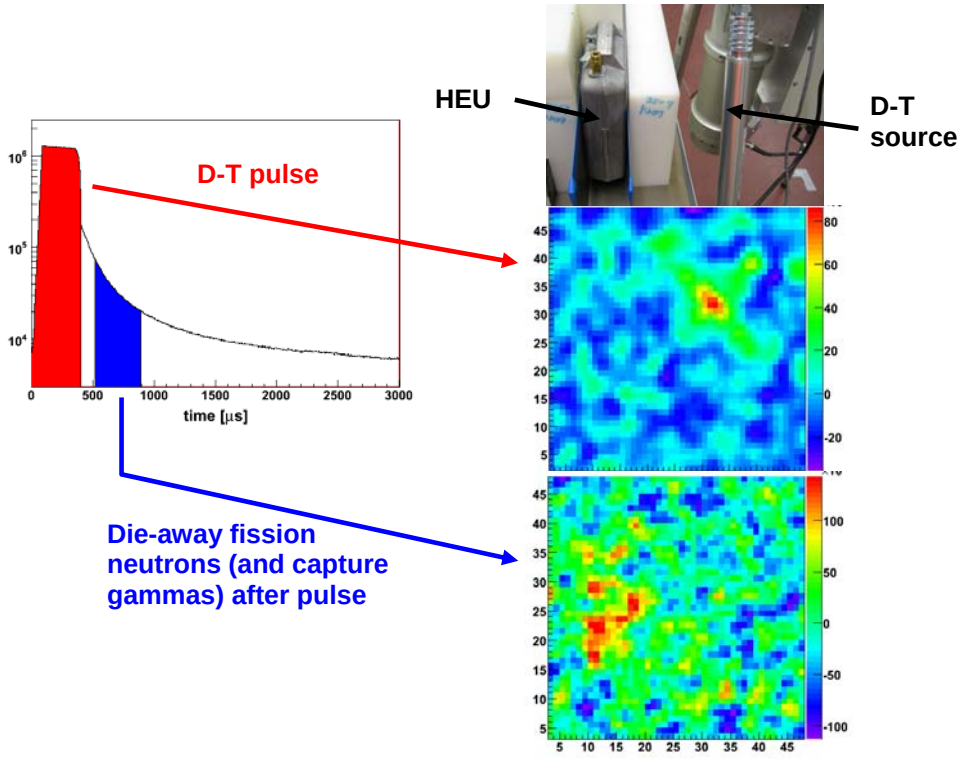

Fig. 6. Active imaging measurement with the D-T generator and clamshell containing HEU. On the left, counts in the imager with respect to D-T generator pulse time are shown with the pulse and die-away imaging regions corresponding to the images on the right highlighted. Because of the large gamma ray background, the statistically noisy die-away image was formed from the difference between measurements with and without HEU.

In these measurements, emanations from the D-T generator and fuel were continuously counted and then sorted in time with respect to the D-T generator pulse. The count rates during the active measurement were much higher than the passive measurements, making imaging of comparatively small signals more difficult. During the interrogating pulse, the imaging array counted at some 2.4×10^6 counts s^{-1}, while during the window used to measure the die-away, the imaging array counted at 7.2×10^4 counts s^{-1}. The minimum rate reached between pulses was 1.3×10^4 counts s^{-1}, a factor of 10 higher than the normal background level in the ZPPR workroom. In the absence of HEU, this background consists entirely of gamma rays within a few microseconds of the end of the interrogation pulse, and poses a formidable background out of which to isolate the comparatively small signal from fast neutrons when HEU is present. Because of the large number of gamma rays associated with the interrogation and the inability of the imaging detector to discriminate between neutrons and gamma rays, the image of the HEU had to be formed from the difference between measurements with and without the HEU present. The measured average signal rate was approximately 165 counts s^{-1}, consistent with a die-away source with a neutron rate of 6.5×10^5 neutrons s^{-1}. Note that this signal rate is three times the rate from

the “I” configuration; however, the large increase in background ensures that the image was dominated by noise. To ensure that the measured signal was a result of induced fissions rather than normal decay activity of the HEU, it was also measured passively to verify that the gamma ray signature from it through the 2.54 cm of lead at the imaging detector was negligible. Although encumbered by high background rates, these measurements demonstrate the ability to image fast neutrons from either differential die-away or delayed neutron-induced fission. However, this capability will only become practical with the development and incorporation of detectors that can discriminate between neutrons and gamma rays. An improved detector with pulse shape discrimination would enable detailed active imaging measurements.

CONCLUSIONS

The present work demonstrates a new capability of coded-aperture fast-neutron imaging with safeguards-relevant sources, both passively with spontaneous fission sources and actively with induced fission sources. The combination of good efficiency and good spatial resolution enable fast-neutron imaging to be useful for a variety of applications where it is desirable to characterize safeguards-relevant sources in situ. This capability can be made practical, particularly in combination with active interrogation, when imaging detectors that can distinguish neutrons from gamma rays are developed.

REFERENCES

1. E. E. Fenimore and T. M. Cannon, “Coded aperture imaging with uniformly redundant arrays,” Appl. Opt., Vol. 17, No. 3, 337–347, 1978.

2. E. E. Fenimore, “Coded aperture imaging: predicted performance of uniformly redundant arrays,” Appl. Opt., Vol. 17, No. 22, 3562–3570, 1978.

3. K.P. Ziock et al., “A fieldable-prototype, large-area, gamma-ray imager for orphan source search,” IEEE-NSS Conference Record, pp. 949–958, 2007.

4. P.E. Vanier and L. Forman, “Forming images with thermal neutrons,” Proc. SPIE, 4784A, pp. 183–193, 2002.

5. F. Habte, M. A. Blackston, P. A. Hausladen, L. Fabris, “Enhancing pixelated fast-neutron block detector performance using a slotted light guide,” IEEE-NSS conference record, pp. 3128–3132, 2008.